ANFIS Control Based improve for a Transient and Voltage Stability of Photovoltaic Inverters microgrid system

[*]Dr. J. Srinu Naick, [#]P. Ashok Kumar

[*]Professor, [#]B.Tech. Student, EEE Department, Chadalawada Ramanamma Engineering College, Tirupati, Andhra Pradesh, India, speaksrinu@gmail.com.

Abstract— the addition of more megawatt-scale photovoltaic (PV) power plants and other large Inverter-based power stations to the electricity system is causing changes in the way the power grid is managed. In response to these developments, new grid code requirements mandate that inverter-based power stations not only stay connected to the grid but also provide Dynamic support. With defective conditions, the integration of renewable-energy power sources such as solar and marine current might have a severe impact on system stability. This paper presents a PV inverter control scheme that improves the transient stability of a synchronous generator connected to the grid controller, using an adaptive-network-based fuzzy inference system (ANFIS) to achieve damping improvement of an overall power system stability problem fed to a Photovoltaic Inverters for Transient and Voltage Stability system. The suggested control approach causes the PV inverter's dc link capacitors to absorb some of the kinetic energy stored in the synchronous machine during temporary halt, as shown in the study. In addition, by injecting reactive power into the system, the proposed method can increase voltage stability.

Keywords: Photovoltaic generation, synchronous machine, transient stability, voltage stability.

I. INTRODUCTION

RE sources, which are typically connected to the power grid through power converters, have significantly more recently been incorporated into power systems (such as inverters). The operation of power systems under intense disturbances is a crucial issue because the growth in PV generation implies some new technical challenges, such as transient stability [1]. This new system configuration has a decreased governor response and overall system inertia, which could have an adverse effect on the SM rotor angle's transient response. However, new opportunities like ancillary services to SMs are made possible by the inverters used in PV generation. For instance, PV inverters may assist in preserving stability following a system disturbance, such as a short circuit brought on by a lightning strike on a transmission line, which may result in the FD signal opening the circuit breakers on the faulted line [2]. The significant changes in the power system configuration regarding the operation of power inverters were not anticipated by the GCs of the previous two decades. Even now, future scenarios of RE generation are challenging to comprehend and estimate. Due to this, GCs have demanded that the RE sources be turned off as soon as a disturbance is found over the past ten years [3]. As long as the level of RE penetration is not significant, which is done to prevent the loss of synchronism, this requirement is acceptable. However, in order to maintain synchronism and voltage stability, the generation unit must not only remain connected to the power system but also provide support. This is because the GCs have changed to require FRT capacity from RE units during disturbances [4]. The PV inverters used in distributed generation units and by PV plants connected to the medium voltage transmission grid must meet additional requirements set forth by some nations. To increase voltage stability, some of these standards permit the use of an MC operating mode or momentarily stop transferring active power to the grid in favour of supporting reactive power [5] [7]. As can be seen in [5], [6], and [8], some GCs establish APRRR for post fault operation. The FRT capacity of PV systems that are compliant with the GCs has been extensively researched in the literature. For instance, [9] proposes a FRT scheme that enables the power quality to adjust based on a tradeoff between power ripple and current harmonics, as required in the German GC [6], to support the grid by injecting reactive power. [10] investigates the effects of the following PV system operating modes on short term voltage stability, post-fault recovery, and ultimately transient stability: grid disconnection, FRT in blocking mode, and FRT with dynamic voltage support. Another pertinent study is presented in [11], which develops a model of the LVRT capacity in PV plants using results from manufacturer-conducted field tests that adhered to the Chinese GC [7]. Finally, [12] adapts a PV plant's

 DOI : 10.35291/2454-9150.2022.0389

control system to include current limiters and dc link voltage control, enabling the FRT capability to handle any fault. A more thorough investigation of the effects that the GC's operating modes have on the system transient stability is still required, despite the fact that the implementation of FRT on PV systems and its advantages for dynamic voltage support have been studied in the literature. The Blue Cut Fire [13] and Canyon 2 Fire [14] incidents demonstrated how little research has been done on the effects of PV systems' MC operating mode on the stability of power systems during transmission faults. To comprehend how MC and post-fault APRRR affect stability, the NERC/WECC joint task force [13], [14] suggests running dynamic simulations. These studies are required to ascertain the circumstances in which the MC should be used, whether it should deliver active or reactive power, and the order in which the injected current should be delivered (positive, negative, or zero). The effect of the MC mode on transient stability has recently been the subject of some research [15], [16]. In order to ensure transient stability, this paper proposes a FRT control scheme based on the absorption of the kinetic energy stored in the rotating mass of the SM. This is because it is crucial to make the PV plant have a positive impact on the system stability while operating in the MC mode. By supplying reactive power to the grid, the proposed ANFIS control scheme also enhances voltage stability and its post-fault recovery. Using the suggested method, the SM active power output is raised to a level that is nearly equal to its pre-fault value. This restores the balance between the SM electrical power and mechanical power, which slows the rotor's rotational speed, which in turn lessens rotor angle excursions and ensures transient stability during the disturbance's initial cycles. The proposed control strategy does not call for any additional hardware in the inverters' dc link or on the power system (as in [17]). (as in [18]). The control scheme presented in this paper performs better than the solutions suggested in [18] and [19], ensuring transient stability in the first cycles following the FD. No new hardware needs to be added to a PV plant's existing hardware in order to implement the proposed control scheme, so no additional costs are anticipated. But it depends on a PMU and a PDC, which might need to be set up. Despite the size of the investment, there is a growing trend toward using smart grid technologies to operate power systems in a cost-effective and coordinated manner. As they offer additional functionalities for metering, monitoring, and control in this environment, PMUs and PDCs might thus turn into commodities.

II. EXISTING CONTROL SCHEME OF THE PV INVERTER

The transient stability analysis that is presented below makes use of the power system configuration that is depicted in Fig. 1. This hybrid power system consists of an SM running concurrently with a PV system, and two transmission lines connect both power plants to the grid. The PV system is made up of n PV units, as shown in Fig. 2. During normal operation, these units are controlled using an MPPT strategy. The PV inverters can, however, enable FRT in MC mode and carry out the suggested ANFIS control action to reduce the SM load angle (δ_r) during a fault in one of the transmission lines.

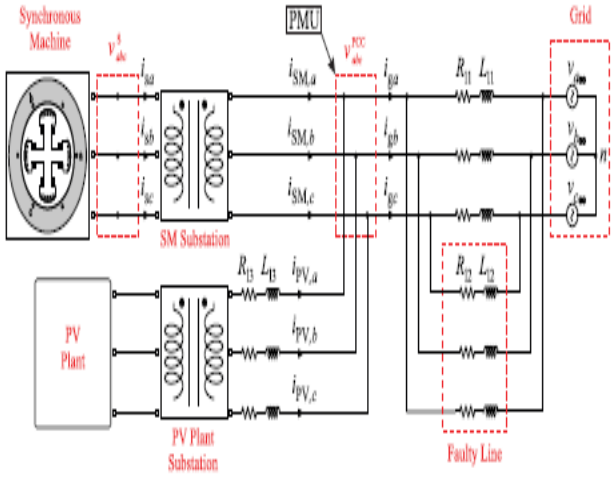

Fig. 1 Three-phase diagram of a utility-scale hybrid power system.

It is common knowledge that an APF can indirectly control grid currents by injecting harmonic components and reactive load current components. Similar to this, the currents that the PV inverters inject into the grid in order to control the torque (or active power) and magnetic flux (or reactive power) can be imposed. This is possible because the SM governor typically acts after the fault has ended, whereas these inverters can act during the fault time frame. By keeping the SM's active power output as close to its pre-fault state as possible, the disequilibrium brought on by a disturbance can be diminished. This means that during a fault, any excess active power that the defective grid is unable to handle must be delivered to the PV units' dc link capacitors. It should be noted that this strategy is dependent on the inverter's operational constraints, which must be taken into account. The goal of the suggested ANFIS control scheme during the fault is to maintain the SM active power (P_{SM}^{f}) at its pre-fault value (P_{SM}^{pre-f}). The reference active power of the PV plant should be in order to accomplish this goal.

$$P_{PV}^{*} = \bar{P}_{g}^{f} - P_{SM}^{pre\text{-}f}, \quad (1)$$

where $\bar{P}_g^f$ is the typical active power added to the grid while the fault was present. The PV plant will need real-time measurements of the SM and the grid, as shown by (1). A PMU is installed in the SM substation to measure the voltage phasor at the PCC and the current phasors of the transmission lines for this purpose, as shown in Fig. 1. The PDC at the PV plant substation will receive synchrophasor data at a rate of up to 120 samples per second using current PMU technology [20], [21]. A PDC

 DOI : 10.35291/2454-9150.2022.0389

is used to combine and time-synchronize the phasor data obtained from one or more PMUs, from other PDCs, and from other sources. For control decision action, the PDC is a crucial link between PMUs and the synchrophasor software programme, which receives the time-synchronized data [21]. The communication delay caused by sampling, data filtering and processing, communication system I/O, and communication distance is a crucial component of data transmission. The PV inverters won't be able to function properly during the delay because no variation in the SM active power output measurement reaches the PDC. As a result, the communication system must be created to prevent delays that are greater than a predetermined threshold, which is established as the greatest delay that does not jeopardise the ability of the suggested control strategy to guarantee transient stability. It was established in this study that the PMU delay shouldn't exceed 20% of the total fault duration. The simulation in Section IV has a maximum delay of 28 ms, which is well within the 20–50 ms range that [20] describes as being typical for a system. Fig. 3 depicts the proposed FRT scheme to be used on the PV inverters[24][25].

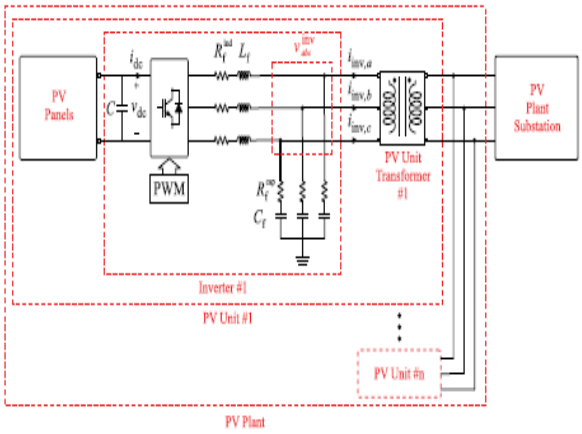

Fig. 2 Three-phase diagram of each PV unit.

Once the PMU measurements are sent to the PV plant substation's PDC, it is possible to compute the power references for each PV unit (Fig. 2) in the PV plant. Based on (1), it is necessary to calculate the pre-fault SM active power during the disturbance. This can be accomplished by using a very slow LPF with a time constant that is much longer than the typical fault duration, of the order of seconds. On the other hand, the control must take into account the decrease in the active power used by the grid. The harmonic and negative-sequence components of the voltages and currents produced by the fault are attenuated using a MAF. The PV reactive power reference calculation follows the same rules. No oscillatory power should be included in the calculation of the reference power for PV plants, according to (1). MAFs and LPFs are employed in order for this to occur during significant grid disturbances. The proposed ANFIS control scheme can track the changes in the average power that is being transferred through the grid because of the higher MAFs cutoff frequency. On the other hand, the SM pre-fault active power output, which serves as a reference signal in the suggested ANFIS control scheme, is kept by using the LPFs with lower cutoff frequencies. The power references of each PV unit are calculated by dividing the reference values through (1), which are for the PV plant, by the number of PV units (n). For safety reasons, the reference P*inv value must be restricted to the highest active power P invmax max that can be absorbed during the disturbance, which can be found by:

$$P_{\max}^{\text{inv}} = \frac{C}{2\Delta t}\left(v_{\text{dc}}^{\max 2} - v_{\text{dc}}^{2}\right), \tag{2}$$

Where vdc is the maximum dc voltage during a disturbance, C is the dc link capacitance, 1t is the maximum fault duration, vdc is the steady state dc link voltage, and C is the dc link capacitance. This imposed restriction on the controller prevents the dc link voltage from rising above the maximum inverter dc input voltage, which is a more stringent restriction than the capacitor's surge voltage of two times its nominal voltage, as in [23]. Additionally, the reference Q*inv needs to stay within the range of the maximum reactive power $Q_{\text{inv}}^{\max}$, which can be calculated as

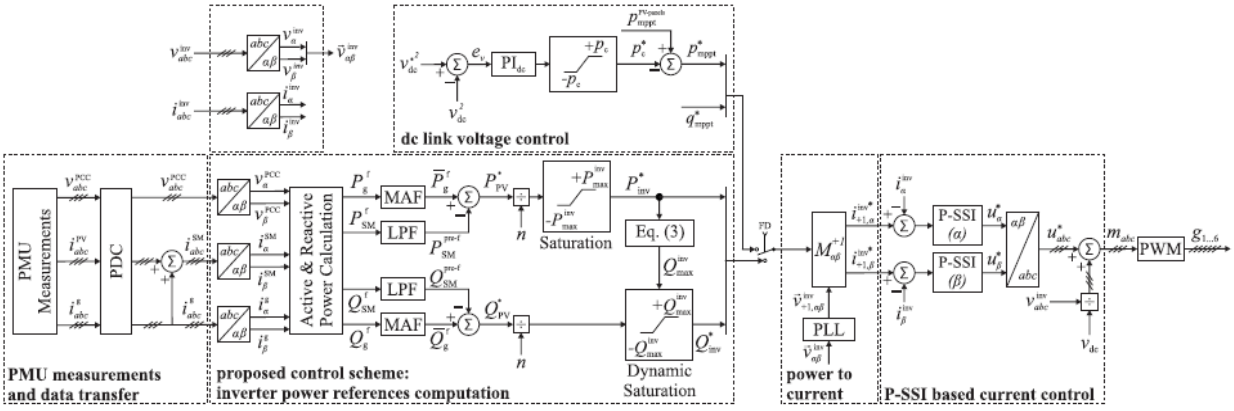

Fig. 3. Proposed FRT scheme including: PMU measurements and data transfer, FRT inverter power references computation, dc link voltage control, and P-SSI based current control.

 DOI : 10.35291/2454-9150.2022.0389

$$Q_{\max}^{\text{inv}} = \sqrt{\left(S_{\max}^{\text{inv}}\right)^2 - \left(P_{\text{inv}}^{*}\right)^2}. \quad (3)$$

It is important to keep in mind that the proposed ANFIS control scheme prioritises the calculation of the active power reference required to be absorbed by the PV units. To improve voltage stability, as required by some GCs [5]–[7], the limit imposed by (2) offers a power margin that can be used as reactive power support. In order to achieve constant power injection, which necessitates synthesising all odd harmonic current components, or oscillatory power injection of frequency 2ω, which necessitates only synthesising fundamental-frequency positive sequence (FFPS) currents, the FRT scheme computes the inverter current references. The oscillatory power injection, when used with the suggested ANFIS control scheme, has no effect on the average SM active power output because its mean value is zero; consequently, it has no impact on the variation of δ_r. Also to be noted is the possibility of exceeding the inverter's maximum short circuit withstand capacity when all odd harmonic currents are injected as opposed to just FFPS currents[26]. For these reasons, the inverter current references used in this research only include the FFPS component. The instantaneous power theory is used to determine the current references in the "power to current" block [24]:

$$\begin{bmatrix} i_{+1,\alpha}^{\text{inv}^*} \\ i_{+1,\beta}^{\text{inv}^*} \end{bmatrix} = M_{\alpha\beta}^{+1} \begin{bmatrix} P_{\text{inv}}^{*} \\ Q_{\text{inv}}^{*} \end{bmatrix}, \quad (4)$$

Where $M_{\alpha\beta}^{+1}$ is given by

$$M_{\alpha\beta}^{+1} = \frac{1}{\left|\vec{v}_{+1,\alpha\beta}^{\text{inv}}\right|^2} \begin{bmatrix} v_{+1,\alpha}^{\text{inv}} & v_{+1,\beta}^{\text{inv}} \\ v_{+1,\beta}^{\text{inv}} & -v_{+1,\alpha}^{\text{inv}} \end{bmatrix}. \quad (5)$$

In equation (5), a PLL is used to determine the FFPS component of the voltage at the PV unit's Terminals ($\vec{v}_{+1\alpha\beta}^{\text{inv}}$) (a GDSC-PLL was used for obtaining the results presented in this paper due to its better performance characteristics [25]). The three-phase current that results ($i_{\text{inv}}^{\text{abc}}$) shouldn't be greater than the inverter unit's datasheet-specified short-circuit withstand capacity [22].

III. VOLTAGE AND CURRENT CONTROLLERS

Figure 3 depicts the total control technique that was implemented. During steady-state operation, the dc link voltage control block makes it possible to transfer the power generated by PV panels to the grid [26]. The dc link voltage controller that is represented in Figure 4 decides the active power reference (p_C^*) that will be given to the capacitor in order to reduce the amount of voltage control error that occurs (ev). This value is a representation of the amount of power that is necessary to keep the voltage of the dc link at a constant value. As shown in Figure 4, the power that is collected from the PV panels by the MPPT ($P_{\text{mppt}}^{\text{PV-panels}}$) added to the total power that is produced by the cell $(p_C^*)'$. As a direct consequence of this, the PV panels $P_{\text{mppt}}^{\text{PV-panels}}$ are incorporated into the active power reference. The maximum amount of power variation that the controller is able to account for is determined by which values are selected for the inferior and superior bounds of the anti-windup saturation block (Figure 4). When $(p_C^*)'$ and $(p_C^*)'$have different values, the integral controller's input is set to zero by the block "= =". When the FD signal is triggered, the "dc link voltage control" block is disabled, which causes the transfer of active power from the PV panels to the grid to enter the MC mode. This mode allows for more efficient use of the available power. Under these conditions, the kinetic energy of the SM can be absorbed by the dc capacitors, which in turn reduces the impact that the fault has on the SM's transient stability. The "P-SSI based current control" block will perform its function to track the current references, $i_{+1\alpha}^{\text{inv}}$;and $i_{+1\beta}^{\text{inv}}$; that are obtained from the "dc link voltage control" block in steady-state operation or from the "proposed ANFIS control scheme" block during the disturbance. During steady-state operation, the "dc link voltage control" block will be responsible for providing these current references. This is accomplished through the utilisation of two controllers that are based on sinusoidal-signal integrators (SSIs), one for the components and the other for the components [27], [28]. In addition, the controller's bandwidth was adjusted by the use of a proportionate action.

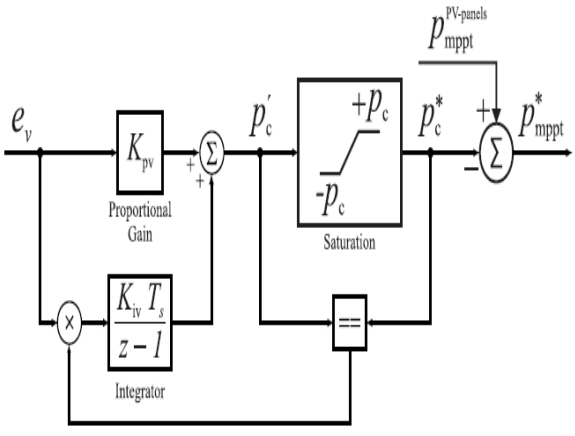

Fig. 4 Diagram of the dc link voltage controller with anti-windup action.

Because of its widespread application in systems with sinusoidal references and/or disturbances, the P-SSI-based current control technique was selected for this project. This is due to the fact that its transfer function is identical to that of a sinusoidal signal; as a result, the steady-state error for sinusoidal reference signals is eradicated (according to the internal model principle). The modulation signals mabc are

 DOI : 10.35291/2454-9150.2022.0389

obtained by adding a feed forward value of $\frac{v_{abc}^{inv}}{v_{dc}}$ dc to the output of the controllers. These signals are then transformed by a PWM into commands (g1... 6) for the IGBTs that are contained within the inverters. The control for the dc voltage needs to move significantly more fast than the control for the current.

IV. Design of an ANFIS Damping Controller for ICR

A. ANFIS Structure:

In this paper, Sugeno-type [31], [32] The learning method and topology of ANFIS are presented. Model-free estimators, neural networks and fuzzy logic [30] both have the capacity to handle uncertainties and noise. Both strategies distribute and parallelize the information into a framework of numbers. As a result, one can change a fuzzy-logic architecture into a neural-network architecture and vice versa. In order to obtain the parameters that would not have been possible in fuzzy-logic architecture, a network created in this way could make use of the excellent training algorithms available to neural networks. Additionally, the network created in this manner would no longer be a mystery because it would be capable of interpreting linguistic variables using fuzzy logic [26]. Like fuzzy systems, ANFIS's network organises two components. While the second part is the conclusion, the first part is the antecedent. Rules in the form of a network connect these two components to one another. If the ANFIS in network structure is shown to have five layers, as in Fig. 5, it can be referred to as a multilayered neural network. The first layer performs a fuzzification process, the second layer performs a fuzzy AND of the antecedent part of the fuzzy rules, the third layer normalises the membership functions (MFs), the fourth layer performs the consequent part of the fuzzy rules, and the final layer computes the output of the fuzzy

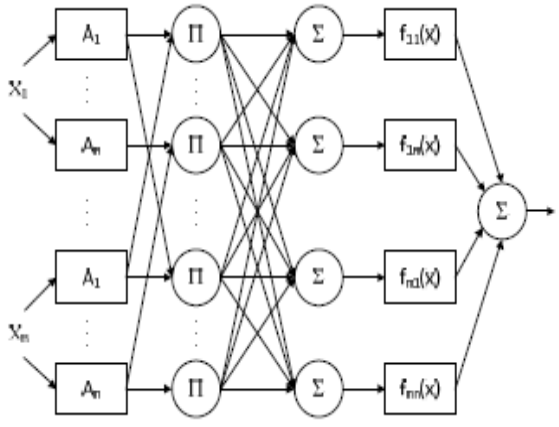

Fig. 5 Typical ANFIS structure

system by adding the fourth layer's outputs. Three inputs and three labels for each input are taken into consideration for the ANFIS structure in Fig. 5. The Sugeno-type structure of an ANFIS is depicted in Fig. 5, where the structure rules are as follows:

$$\text{If } (x_1 = A_i) \text{ and } (x_2 = B_i) \text{ and } (x_3 = C_i)$$
$$\text{then } (f_i = p_i x_1 + q_i x_2 + r_i x_3 + s_i)$$

where the inputs are,, and ; the fuzzy sets are,, and ; the outputs are within the fuzzy region designated by the fuzzy rule ; the designed parameters are,,, and ; and the number of MFs of each input is.

B. Learning Algorithms:

The ANFIS learning technique's fundamental concept is very straightforward and offers a method for fuzzy modelling to acquire knowledge about a data set in order to compute the MFs to track the provided input/output data, which function similarly to neural networks. It is a key training procedure for fuzzy inference systems of the Sugeno type. In order to determine the parameters of Sugenotype fuzzy inference systems, ANFIS employs a hybrid learning algorithm. The membership function parameters of fuzzy inference systems are trained using a combination of the least-squares method and the back-propagation gradient descent method [20] to mimic a given training data set.

C. Design of the Proposed ANFIS Damping Controller:

The ANFIS damping controller is designed in this section using the ANFIS control theorem technique. The rotor-speed deviation of the SG ($\Delta_{\omega sG}$), the active-power deviation of the onshore PV system (ΔP_{pv}), and the active-power deviation of the combined PMSG-based OWF and SCIG-based MCF ($\Delta P_{WF/MCF}F$)) are used as inputs when designing the ANFIS controller. They were selected as the input variables because the main power sources in the system under study are the SG-based power system, PV system, wind farms, and marine current farms. These power sources exhibit both significant oscillations and power fluctuations.

When compared to the other cases, the effectiveness of various feedback signals for the ANFIS damping controller will be higher. The oscillations of each feedback signal's own power generation are highly dependent on one another. The ANFIS damping controller receives these input signals in order to produce the modulated control input needed to control. The fuzzy MFs use the three input variables to calculate the stabilising signal of the ANFIS damping controller. The proposed ANFIS approach is implemented using the MATLAB ANFIS-Editor. In a traditional fuzzy approach, the model designer fixes the MFs and the ensuing models based on prior knowledge. The components of a fuzzy system (membership and consequentmodels) can be represented in a parametric form and the parameters are tuned by neural networks if this set is not available but a set of input-output data is observed from the process instead. The fuzzy system then evolves into an ANFIS system. The fuzzy controller performs well and computes output using 343 rules and 7MFs for each variable. Seven linguistic

 DOI : 10.35291/2454-9150.2022.0389

variables—NB (Negative Big), NM (Negative Medium), NS (Negative Small), ZR (Zero), PS (Positive Small), PM (Positive Medium), and PB—are used in this study for each input variable (Positive Big). For the output variable, there are seven additional linguistic variables: IB (Increase Big), IM (Increase Medium), IS (Increase Small), KV (Keep Value), DS (Decrease Small), DM (Decrease Medium), and DB (Decrease Big). For the ANFIS controller, three input variables ($\Delta_{\omega sG}$, $\Delta P_{WF/MCF}$, and ΔP_{pv}) are used. The main goal of using ANFIS learning is to extract a more manageable set of rules, and the same procedures are used[17][19].

Data Generation: A set of three-dimensional input vectors and the corresponding set of one-dimensional output vectors are needed in order to design the ANFIS controller. The input variables,,, and, were uniformly sampled to create the training data, and the value of the stabilising signal was calculated for each sampled point.

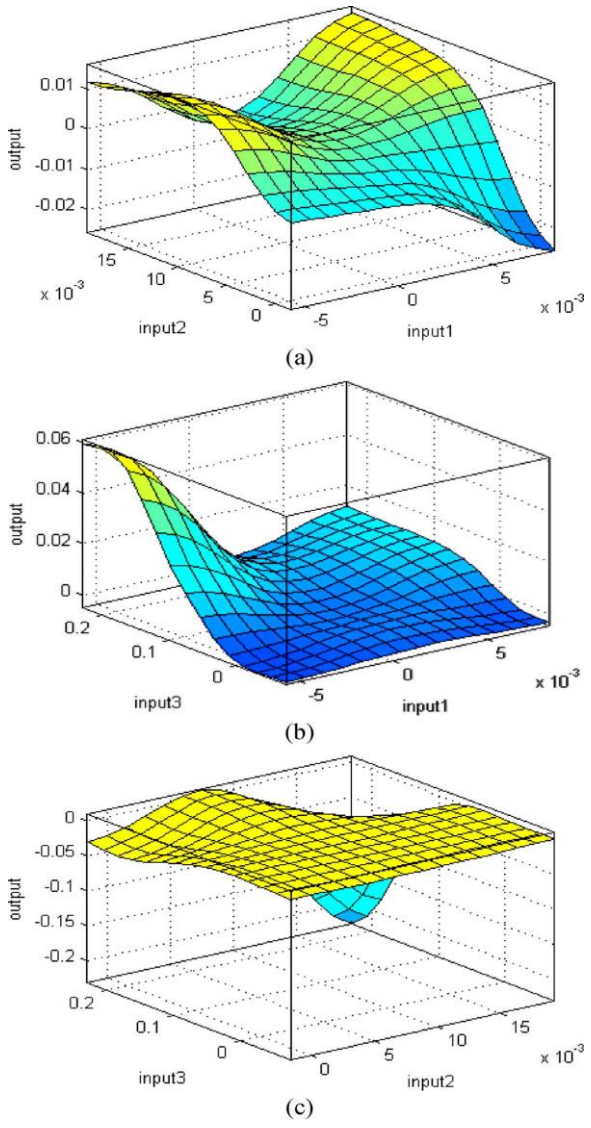

Fig. 6. Control surfaces of the proposed ANFIS model.

Rule Extraction and MFs: Estimating the initial rules comes after producing the data. The rules are extracted after using the subtractive clustering algorithm [21]. The identified studied system is not as closely related to these rules. Consequently, these rules need to be optimised. After obtaining the fuzzy inference system by subtracting clustering, the aforementioned parameters are trained using a hybrid learning algorithm. This algorithm uses back-propagation to iteratively learn the parameter of the premise MFs and linear least-square estimation to optimise the parameters of the ensuing equations.

Training and Testing: The training is continued until the error measured becomes constant.

Results: On a range of linear and nonlinear processes, the ANFIS learning has been put to the test. Here, the goal is to demonstrate that the ANFIS damping controller can perform at the same level as the original one despite having fewer rules and MFs (system with 49 rules). Results for a system with 25 rules and a system with an optimised rule base are reported to show the effectiveness of the suggested combination. The computation becomes quick and uses less memory after the rules are reduced. Fig. 7 depicts the ANFIS structure for the ICR. Figure 6 depicts the control surfaces for the input and output signals, labelled input1, input2, input3, and output, respectively. This study employs the ANFIS toolbox in MATLAB and selects Gauss, 10 epochs, and Hybrid (i.e., mixed least squares and back-propagation) as the MF type, number of epochs, and learning algorithm, respectively. ANFIS can use If-Then rules and can tune the model through MFs thanks to a ten-fold cross-validation method with 280 features to test the model's generalizability. The transient responses of the investigated system with the specified PID damping controller subject to a three-phase short-circuit fault occurring at bus A are used as the training data for the ANFIS. The number of nodes, number of linear parameters, number of nonlinear parameters, total number of parameters, number of training data pairs, and number of fuzzy rules are the parameters of the ANFIS after training. After training and testing, the averaged ten-fold cross validation test results produced 0.0164012 errors, or 1.6 percent of the total. The accuracy of the result is 8.4 percent.

V. SIMULATION RUSULTS AND DISCUSSION OF INVERTER WITH THE PROPOSED ANFIS CONTROL SCHEME AND REACTIVE POWER SUPPORT

The proposed ANFIS control scheme was implemented to include reactive power support in the simulation results (Fig. 7). The findings demonstrate that, in comparison to the second experiment, the PCC voltages rise, as was already predicted given the reactive power support. With this solution, the inverter is able to absorb less active power, resulting in a lower maximum dc voltage of 334.9 V. The oscillations of the SM active power output are

 DOI : 10.35291/2454-9150.2022.0389

higher in the emulated fault than in the second experiment, but they still hover around the pre-fault value. As seen in Fig. 8, the reactive power support draws a higher output inverter current than the inverter current obtained in the second experiment, which when combined with the negative sequence voltages at the PCC results in higher oscillations in the SM active power. When compared to the simulation results, the post-fault oscillations are further diminished.

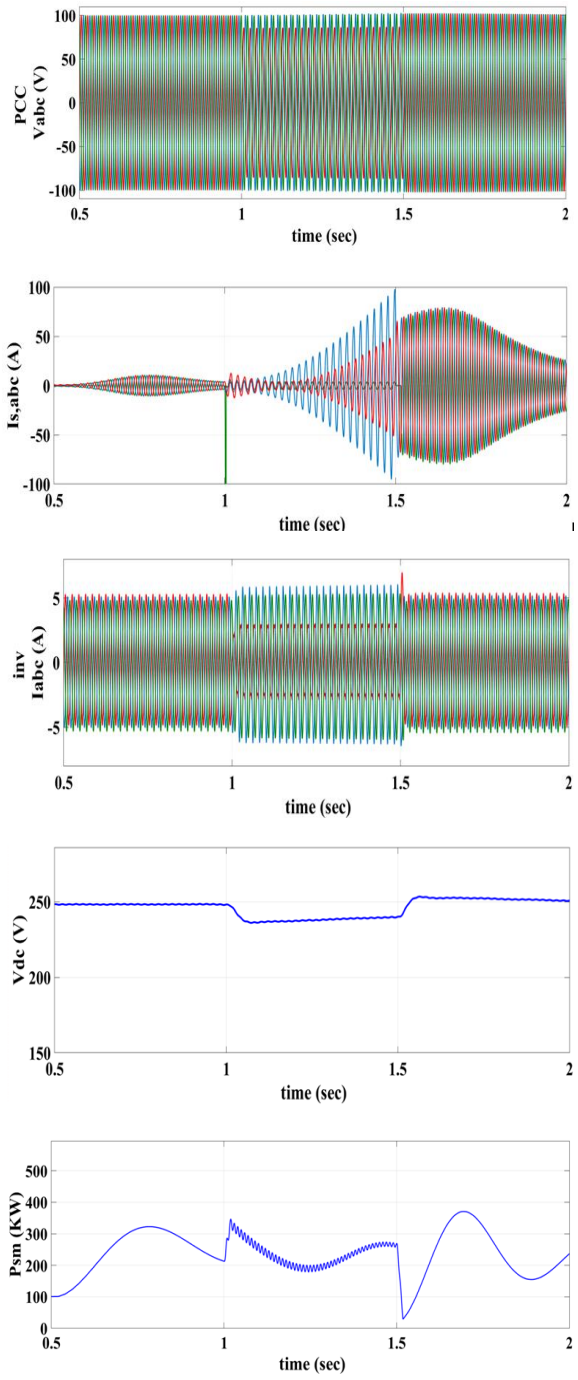

Fig. 7 Simulation results showing the performance of the proposed ANFIS control. Results obtained for: inverter with the proposed ANFIS control scheme and reactive power support.

VI. SIMULATION RESULTS OF TRANSIENT HYBRID SYSTEM

The simulation results shown in Fig. 8 represent a comparison of the transient responses of the following FRT schemes: the PV plant that complies with German GC requirements; the FLC with a VR-FCL installed between the PCC and the transmission grid through an isolation transformer as shown in [17]; and the proposed ANFIS control scheme. Fig. 8a displays the SM active power transient response.

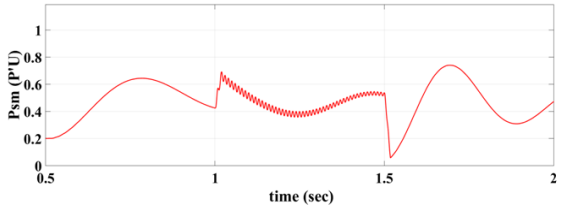

Fig. 8 Comparative responses of the hybrid system subjected to a 2LG fault for SM active power output.

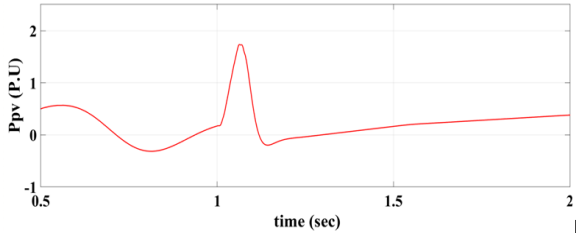

Fig. 9 Comparative responses of the hybrid system subjected to a 2LG fault for PV system active power output

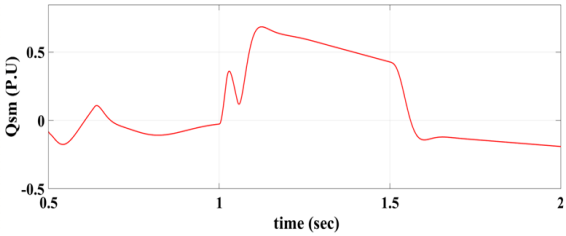

Fig. 10 Comparative responses of the hybrid system subjected to a 2LG fault for SM reactive power output

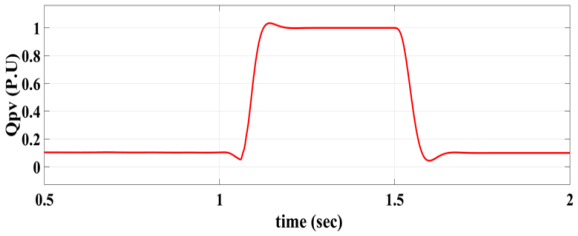

(d)

Fig. 11 Comparative responses of the hybrid system subjected to a 2LG fault for PV system reactive power output.

The results from the German GC and the FLC indicate a notable decline during the fault, which results in an imbalance between electrical and mechanical power. With the exception of the PMU communication delay, the proposed ANFIS control performs better during the fault, increasing the SM active power close to its pre-fault value. Fig. 8b displays the active power transient response of the PV system. The FLC strategy exhibits no appreciable differences before, during, or after the fault. In order to provide reactive power support during the fault, the German GC reduces its output of active power. The active power is

 DOI : 10.35291/2454-9150.2022.0389

recovered after the selected APRRR when using the proposed ANFIS control scheme, in contrast. It should be noted that following the fault, the PV system's active power briefly increases after a higher ramp. This occurs as a result of the capacitor's stored energy being released into the grid, which is also reflected in the PV system's output currents, as shown in Fig. 9c. When compared to the outcomes of the FLC strategy, the German GC does not reduce the SM reactive power output during the fault despite the reactive power support from the PV system. However, as can be seen in Fig. 8c, the proposed ANFIS control scheme reduced it roughly from 70 Mvar (0.7 p.u.) to 50 Mvar (0.5 p.u.). Only the proposed ANFIS control strategies and the GermanGC have established the reactive power support. As a result, the results obtained using the German GC requirements, as shown in Fig. 8d, injected 66 Mvar (0.66 p.u.) of reactive power. The proposed ANFIS control scheme, which injects 98.7 Mvar (0.98 p.u.) into the PCC and allows for higher reactive power support, has been shown to be helpful for both the voltage recovery before and after the fault. The proposed ANFIS control scheme's reactive power support also reveals a slight improvement in the voltage at the PCC during the fault. When compared to the other FRT strategies, it has a very quick voltage recovery after the fault, though. The DC link voltage results in Fig. 8b demonstrate that the DC voltage is maintained near the pre-fault value by both the FLC and German GC strategies. Due to the absorption of active power into the dc capacitors, an increase of up to 1340 V (1.22 p.u.) is seen for the proposed ANFIS control. However, this increase does not exceed the imposed limit of 1500 V, meaning it does not endanger the operation of the inverters. The FLC strategy can restrict the inverters' output currents during a fault, but the proposed ANFIS control scheme and the German GC produce better outcomes in this area. It is important to remember that no strategy goes over the short-circuit withstand limit. The transient responses of the SM rotor angle. According to the German GC, the FLC strategy's maximum rotor angle value was reduced by 12.5%. The maximum (δ_r) value reached by the FLC strategy is significantly reduced by 48 percent in the proposed ANFIS control scheme. Due to the inverters' active power recovery, it is important to note that post-fault rotor angle oscillations when the proposed ANFIS control scheme is implemented are higher than those obtained from the FLC and German GC strategies.

VII. CONCLUSION

This paper has presented the transient and voltage stability of a grid and PV inverter, as well as SG-based hybrid power systems. A PID damping controller and an ANFIS damping controller for hybrid power systems have been created to achieve power-fluctuation mitigation and damping improvement for the examined system. The developed ANFIS damping controller has three input variables, whereas the PID damping controller only has one. Comparative time-domain simulations of the examined system subjected to a three-phase short-circuit fault can act when the PV system is in MC mode, assisting the grid in regaining stability during and after a transmission grid disruption. To provide transient stability, the ANFIS control method causes the SM kinetic energy to be absorbed by the dc link capacitors. It also allows for the injection of reactive electricity into the grid to help maintain voltage stability. Simulation results show that the suggested control strategy efficiently ensures the SM's transient stability by reducing rotor angle oscillations within the initial few cycles of the failure. In compared to other FRT control techniques, it has shown improvements in grid voltages during the fault period and a very quick post-fault voltage recovery.

REFERENCES

[1] M. Milligan, B. Frew, B. Kirby, M. Schuerger, K. Clark, D. Lew, P. Denholm, B. Zavadil, M. O'Malley, and B. Tsuchida, ``Alternatives no more: Wind and solar power are mainstays of a clean, reliable, affordable grid," IEEE Power Energy Mag., vol. 13, no. 6, pp. 78fi87, Nov. 2015.

[2] N. W. Miller, ``Keeping it together: Transient stability in a world of wind and solar generation," IEEE Power Energy Mag., vol. 13, no. 6, pp. 31fi39, Nov. 2015.

[3] IEEE Standard for Interconnecting Distributed Resources With Electric Power Systems, IEEE Standard 1547-2003, Jul. 2003.

[4] W. Weisheng, C. Yongning, W. Zhen, L. Yan, W. Ruiming, N. Miller, and S. Baozhuang, ``On the road to wind power: China's experience at managing disturbances with high penetrations of wind generation," IEEE Power Energy Mag., vol. 14, no. 6, pp. 24fi34, Nov. 2016.

[5] IEEE Standard for Interconnection and Interoperability of Distributed Energy Resources With Associated Electric Power Systems Interfaces, IEEE Standard 1547-2018, Apr. 2018.

[6] Technical Requirements for the Connection and Operation of Costumer Installations to the High-Voltage Network (TCC High-Voltage), Standard VDE-AR-N 4120, Jan. 2015.

[7] Technical Requirements for Connecting Photovoltaic Power Station to Power System, Standard Chinese Grid Code GB/T 19964-2012, Jun. 2013.

[8] National Grid, Guidance NotesfiPower Park Modules, National Grid, National Grid House, Warwick Technology Park, Warwick, U.K., no. 3, 2012.

[9] F. A. S. Neves, M. Carrasco, F. Mancilla-David, G. M. S. Azevedo, and V. S. Santos, ``Unbalanced grid fault ride-through control for singlestage photovoltaic inverters," IEEE Trans. Power Electron., vol. 31, no. 4, pp. 3338fi3347, Apr. 2016.

[10] G. Lammert, D. Premm, L. D. P. Ospina, J. C. Boemer, M. Braun, and T. Van Cutsem, ``Control of photovoltaic systems for enhanced short-term voltage stability and recovery," IEEE Trans. Energy Convers., vol. 34, no. 1, pp. 243fi254, Mar. 2019.

[11] P. Chao, W. Li, S. Peng, X. Liang, D. Xu, L. Zhang, N. Chen, and Y. Sun, ``A unified modeling method of photovoltaic generation systems under balanced and unbalanced voltage

 DOI : 10.35291/2454-9150.2022.0389

dips," IEEE Trans. Sustain. Energy, vol. 10, no. 4, pp. 1764fi1774, Oct. 2019.

[12] M. Mirhosseini, J. Pou, and V. G. Agelidis, ``Single- and two-stage inverter-based grid-connected photovoltaic power plants with ride-through capability under grid faults," IEEE Trans. Sustain. Energy, vol. 6, no. 3, pp. 1150fi1159, Jul. 2015.

[13] 1200 MW Fault Induced Solar Photovoltaic Resource Interruption Distur- bance Report: Southern California Event: August 16, 2016, North Amer. Electr. Rel. Corp., Atlanta, GA, USA, 2017.

[14] 900 MW Fault Induced Solar Photovoltaic Resource Interruption Distur- bance Report: Southern California Event: October 9, 2017, North Amer. Electr. Rel. Corp., Atlanta, GA, USA, Feb. 2018.

[15] H. Shin, J. Jung, S. Oh, K. Hur, K. Iba, and B. Lee, ``Evaluating the infiuence of momentary cessation mode in inverter-based distributed generators on power system transient stability," IEEE Trans. Power Syst., vol. 35, no. 2, pp. 1618fi1626, Mar. 2020.

[16] H. Shin, J. Jung, and B. Lee, ``Determining the capacity limit of inverterbased distributed generators in high-generation areas considering transient and frequency stability," IEEE Access, vol. 8, pp. 34071fi34079, Feb. 2020.

[17] M. K. Hossain and M. H. Ali, ``Transient stability augmentation of PV/DFIG/SG-based hybrid power system by nonlinear control-based variable resistive FCL," IEEE Trans. Sustain. Energy, vol. 6, no. 4, pp. 1638fi1649, Oct. 2015.

[18] L. Wang, Q.-S. Vo, and A. V. Prokhorov, ``Stability improvement of a multimachine power system connected with a large-scale hybrid windphotovoltaic farm using a supercapacitor," IEEE Trans. Ind. Appl., vol. 54, no. 1, pp. 50fi60, Jan. 2018.

[19] M. Edrah, K. L. Lo, and O. Anaya-Lara, ``Impacts of high penetration of DFIG wind turbines on rotor angle stability of power systems," IEEE Trans. Sustain. Energy, vol. 6, no. 3, pp. 759fi766, Jul. 2015.

[20] IEEE Standard for Synchrophasor Data Transfer for Power Systems, IEEE Standard C37.118.2, Dec. 2011.

[21] G. Dileep, ``A survey on smart grid technologies and applications," Renew. Energy, vol. 146, pp. 2589fi2625, Feb. 2020.

[22] ABB Central Inverters. PVS980-58 Central InvertersfiHardware Manual. Accessed: Feb. 10, 2021. [Online].Available:https://new.abb.com/news/detail/23761/abb-launches-next-generation-central-inverterwith- unique-cooling-capabilities

[23] AVX. (Jun. 2015). FFLC Series Film Capacitors. http://www.avx.com/products/film-capacitors/medium-power-filmcaps/ ffic/ [24] H. Akagi, S. Ogasawara, and H. Kim, ``The theory of instantaneous power in three-phase four-wire systems: A comprehensive approach," in Proc. Conf. Rec. IEEE Ind. Appl. Conf. 34th IAS Annu. Meeting, vol. 1, Oct. 1999,pp. 431fi439.

[25] F. A. S. Neves, M. C. Cavalcanti, H. E. P. D. Souza, E. J. Bueno, and M. Rizo, ``A generalized delayed signal cancellation method for detecting fundamental-frequency positive-sequence three-phase signals," IEEE Trans. Power Del., vol. 25, no. 3, pp. 1816fi1825, Jul. 2010.

[26] P. S. N. Filho, T. A. D. S. Barros, M. V. G. Reis, M. G. Villalva, and E. R. Filho, ``Strategy for modeling a 3-phase grid-tie VSC with LCL filter and controlling the DC-link voltage and output current considering the filter dynamics," in Proc. IEEE 16th Workshop Control Modeling PowerElectron. (COMPEL), Jul. 2015, pp. 1fi8.

[27] L. Limongi, R. Bojoi, G. Griva, and A. Tenconi, ``Digital current-control schemes," IEEE Ind. Electron. Mag., vol. 3, no. 1, pp. 20fi31, Mar. 2009.

[28] R. C. Neto, F. A. Neves, and H. E. D. Souza, ``Complex controllers applied to space vectors: A survey on characteristics and advantages," J. Control,Automat. Elect. Syst., vol. 31, no. 5, pp. 1132fi1152, Jul. 2020.

[29] P. S. Flannery and G. Venkataramanan, ``A fault tolerant doubly fed induction generator wind turbine using a parallel grid side rectifier and series grid side converter," IEEE Trans. Power Electron., vol. 23, no. 3, pp. 1126fi1135, May 2008.

[30] A. Mullane, G. Lightbody, and R. Yacamini, ``Wind-turbine fault ride-through enhancement," IEEE Trans. Power Syst., vol. 20, no. 4,pp. 1929fi1937, Nov. 2005.

[31] J. Chen, L. Jiang, W. Yao, and Q. H. Wu, ``Perturbation estimation based nonlinear adaptive control of a full-rated converter wind turbine for fault ride-through capability enhancement," IEEE Trans. Power Syst., vol. 29, no. 6, pp. 2733fi2743, Nov. 2014.

[32] T. Takagi and M. Sugeno, "Fuzzy identification of systems and its application to modeling and control," IEEE Trans. Syst., Man, Cybern., vol. SMC-15, no. 1, pp. 116–132, Jan./Feb. 1985.

AUTHORS PROFILE

Dr.J.Srinu Naick received his B.E degree in Electrical & Electronics Engineering from Andhra University Vishakhapatnam AP, India in 2003 and M.Tech with Energetics from NIT Calicut, Calicut, and Kerala, India in 2007. Ph.D with power system from Achiryanagarjuna university in 2019 He is having 18 years of teaching and research experience. He is currently working as Professor in the Department of EEE, Chadalawada Ramanamma Engineering College (Autonomous), JNTUA, Tirupati, Andhra Pradesh, India. His areas of interest are in the Power systems Industrial Drives & FACTS Controllers.

P. Ashok Kumar is an Under Graduate student studying IV B.Tech Electrical and Electronics Engineering from Chadalawada Ramanamma Engineering College, Tirupati, Chittoor, A.P, India. His research interests include Power System and

 DOI : 10.35291/2454-9150.2022.0389